Molecular Plant Pathology

MOLECULAR PLANT PATHOLOGY (2012) **13**(9), 1149–1155 DOI: 10.1111/J.1364-3703.2012.00823.X

Short communication

# Transposition of the miniature inverted-repeat transposable element *mimp1* in the wheat pathogen *Fusarium culmorum*

FRANCESCA SPANU[1], MATIAS PASQUALI[2], BARBARA SCHERM[1], VIRGILIO BALMAS[1], ANGELA MARCELLO[1], GIUSEPPE ORTU[3], MARIE DUFRESNE[4], LUCIEN HOFFMANN[2], MARIE-JOSÉE DABOUSSI[3] AND QUIRICO MIGHELI[1,*]

[1]*Dipartimento di Agraria – Sezione di Patologia Vegetale ed Entomologia and Centro interdisciplinare per lo sviluppo della ricerca biotecnologica e per lo studio della biodiversità della Sardegna e dell'area Mediterranea, Università degli Studi di Sassari, Via E. De Nicola 9, I-07100 Sassari, Italy*

[2]*Environment and Agro-biotechnologies Department, Centre de Recherche Public Gabriel Lippmann, 41, rue du Brill, L-4422 Belvaux, Luxembourg*

[3]*Institut de Génétique et Microbiologie, Université Paris Sud 11, Bâtiment 400, F-91405 Orsay Cedex, France*

[4]*Institut de Biologie des Plantes, Université Paris Sud 11, Bâtiment 630, F-91405 Orsay Cedex, France*

## SUMMARY

High-throughput methods are needed for functional genomics analysis in *Fusarium culmorum*, the cause of crown and foot rot on wheat and a type B trichothecene producer. Our aim was to develop and test the efficacy of a double-component system based on the ability of the *impala* transposase to transactivate the miniature inverted-repeat transposable element *mimp1* of *Fusarium oxysporum*. We report, for the first time, the application of a tagging system based on a heterologous transposon and of splinkerette-polymerase chain reaction to identify *mimp1* flanking regions in the filamentous fungus *F. culmorum*. Similar to previous observations in *Fusarium graminearum*, *mimp1* transposes in *F. culmorum* by a cut-and-paste mechanism into TA dinucleotides, which are duplicated on insertion. *mimp1* was reinserted in open reading frames in 16.4% (i.e. 10 of 61) of the strains analysed, probably spanning throughout the entire genome of *F. culmorum*. The effectiveness of the *mimp1/impala* double-component system for gene tagging in *F. culmorum* was confirmed phenotypically for a putative aurofusarin gene. This system also allowed the identification of two genes putatively involved in oxidative stress-coping capabilities in *F. culmorum*, as well as a sequence specific to this fungus, thus suggesting the valuable exploratory role of this tool.

*Fusarium culmorum* (W.G. Smith) Sacc. is a ubiquitous soil-borne fungus able to cause crown and foot rot (CFR) and Fusarium head blight (FHB), especially on durum wheat (Beccari *et al*., 2011; Wagacha and Muthomi, 2007). *Fusarium culmorum* produces type B trichothecenes, such as deoxynivalenol (DON) and nivalenol, as well as the myco-oestrogen zearalenone. Mycotoxins that are present in food and feed at high concentrations may cause serious poisoning in humans and animals (Goswami and Kistler, 2004; Sudakin, 2003). Recently, Scherm *et al*. (2011) have reported that DON plays an important role in CFR severity caused by *F. culmorum*.

Currently, the genome of *F. culmorum* is being sequenced (H. Kosack, Plant Pathology and Microbiology Department, Rothamsted Research, Harpenden, UK, personal communication) but, for many genes, their function is as yet unknown. Its genome seems to consist of more than 10 000 genes distributed over five chromosomes. Therefore, a high-throughput strategy for gene identification and for functional genomics analysis is needed. Moreover, *F. culmorum* is a haploid filamentous fungus with no known sexual stage (Mishra *et al*., 2003), and random insertional mutagenesis and target gene mutation have been successfully used because the mutation of only one allele has an immediate effect on the phenotype.

We decided to adopt a system for random insertional mutagenesis using the heterologous transposon *mimp1*. This element has been identified in *F. oxysporum* (Hua-Van *et al*., 2000), shows terminal inverted repeats (TIRs) like the *impala* transposon and belongs to the *Tc1/mariner* superfamily. *mimp1* does not have a transposase gene and is therefore unable to move autonomously (Hua-Van *et al*., 2000).

Recently, a double-component transposon tagging system based on the *mimp1* element trans-mobilized by the transposase of *impala* has shown exciting results in *Fusarium graminearum*. The reinsertion frequency of *mimp1* was about 83–91% within or next to open reading frame (ORF)/genes (Dufresne *et al*., 2007, 2008). Our aim was to evaluate the functionality and effectiveness of the double-component system *mimp1/impala* in *F. culmorum*.

The MCf 21 nit1 nitrate reductase-deficient mutant (*nia*$^{-}$ phenotype, i.e. sparse mycelium on minimal medium containing sodium nitrate as sole nitrogen source, or MM-nitrate; Scherm *et al*., 2011) was co-transformed with the plasmid pNm1H18, carrying the nonautonomous *mimp1* element located in the first intron of the heterologous *niaD* gene of *Aspergillus nidulans*

*Correspondence: Email: qmigheli@uniss.it

(Malardier *et al*., 1989), and with the plasmid pHEO62, which carries the *impalaE* transposase cloned between the *gpdA* promoter and the *trpC* terminator of *A. nidulans*, with the *hph* selectable marker conferring resistance to hygromycin B (Dufresne *et al*., 2007) (Fig. S1, Supporting information). Hygromycin B-resistant transformants were checked for integration of pNm1H18 using the primers niaD144 and niaD754r (Dufresne *et al*., 2007) (Table S1, Supporting Information). Thirty-eight of 56 transformants had the *mimp1/impala* construct co-integrated into their genome, showing an identical *nia*$^-$ phenotype to *F. culmorum* MCf 21 nit1 when grown on MM-nitrate. The excision of the transposable element allowed the re-acquisition of nitrate reductase function and the *nia*$^+$ colonies (referred to as 'revertant' strains) were easily detected as patches of aerial mycelium with a wild-type phenotype. Selection for monocopy hygromycin B-resistant *mimp1/impala* co-transformants and identification of excision/reinsertion events were pre-screened by polymerase chain reaction (PCR) and confirmed by Southern blotting experiments (Table S1). Only co-transformant M7 among the 38 tested in the pre-screening integrated a single copy of the *niaD::mimp1* construct as shown by PCR (Fig. S2, Supporting Information). The frequency of excision events, observed in independent phenotypic assays on MM-nitrate amended with 50 μg/μL hygromycin B, was about 5–15 revertants/plate. Southern blot analysis confirmed the monocopy insertion and correlated the nia$^+$ phenotype in 11 M7-derived revertants with the excision of *mimp1* (Fig. 1A).

A total of 1300 revertants was generated from M7. Among them, 63 randomly chosen revertants obtained from the M7 co-transformant were checked by specific PCR with primers mi1 and SacF to estimate the rate of reinsertion frequency (Table S1). In 97% of the tested cases (61 of 63 revertants), *mimp1* transposed into different genome sites. PCR results were confirmed by Southern blotting analysis for 11 revertants. Hybridization with the *mimp1* probe indicated when an excision event was followed by the reinsertion of the *mimp1* element. The different sizes of *Xba*I fragments hybridizing with the *mimp1* probe confirmed the independence of reinsertion events (Fig. 1B).

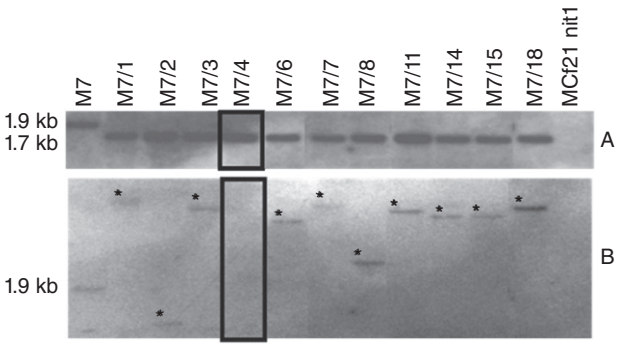


**Fig. 1** Southern blot analysis of revertants *mimp1/impala*. Genomic DNA of co-transformant M7 and derived revertants was digested by *Xba*I and membranes were successively probed with: (A) a 419-bp-long *niaD* probe obtained by polymerase chain reaction (PCR) on the pAN301 plasmid using primers niaCG1 and niaCG2; and (B) a 120-bp-long *mimp1*-specific probe amplified from the pNm1H18 plasmid using the primers mi1 and SacF. The revertants showed a single *niaD* band of 1.7 kb, i.e. 224 bp shorter than the corresponding band of the co-transformant (approximately 1.9 kb), thereby demonstrating the excision of *mimp1* from the nitrate reductase gene (A). The asterisks indicate reinsertion events of the *mimp1* element. In lane 5 (black rectangle), the excision of *mimp1* was not followed by a reinsertion event (B).

To monitor the transposition of *mimp1*, splinkerette-PCR (sp-PCR; Potter and Luo, 2010) was applied for the first time in the filamentous fungus *F. culmorum* to identify and clone the *mimp1* flanking sequences. Briefly, genomic DNA (2.5 μg) was digested at 37 °C for 4 h with 25 units of *Bam*HI or *Bgl*II restriction enzyme (New England Biolabs, Beverly, MA, USA) in a final volume of 50 μL. These enzymes do not cut within the *mimp1* sequence. After purification by spin columns (QIAquick PCR Purification Kit, Qiagen S.p.A., Milan, Italy; not necessary for *Bgl*II), 35 μL of the digestion were ligated to annealed splinkerette oligonucleotide with T4 DNA ligase (New England Biolabs) at room temperature for at least 2 h. After ligation, nested PCR was carried out directly according to Potter and Luo (2010) using Phusion® High-Fidelity PCR Master Mix with HF Buffer (M0531L) (Table S2, Supporting Information). The sp-PCR set after digestion with *Bgl*II showed an efficiency of 71% (43 of 61), whereas, using *Bam*HI, the digestion efficiency was slightly lower (33 of 61). The average size of *Bgl*II splinkerette products was 1700 bp, whereas it was 1000 bp with *Bam*HI.

*mimp1* distribution was estimated based on the similarity with the *F. graminearum* genome, the *F. culmorum* genome being unavailable to date. The absence of 'hot spots', recently detected also in the mobilization of the element *imp160::pyrG* in 200 *niaD* revertants of *A. fumigatus* (Carr *et al*., 2010), increases the efficiency of this system in *F. culmorum*. This is in contrast with the results obtained in *F. graminearum*, where a previous analysis of 91 independent transposition events revealed that the *mimp1* element reinserted in a single locus on chromosome 2 for 19 times (Dufresne *et al*., 2008).

Comparison of the GC content of *mimp1* flanking sequences in *F. culmorum* (minimum, 40.9%; maximum, 58.0%; average, 47.9%) and of the homologous sequences in *F. graminearum* (minimum, 42.3%; maximum, 58.3%; average, 48.0%; Table S3, Supporting Information) suggests no insertional preference for GC-rich regions.

We confirmed that *mimp1* transposes in *F. culmorum* by a 'cut-and-paste' mechanism into TA dinucleotides, which are duplicated on insertion in all sites sequenced (Fig S3A,B, Supporting Information).

Bioinformatics analysis showed that *mimp1* had reinserted within genic regions in 23% (i.e. 14 of 61) of the flanking sequences analysed, namely 10 times within an ORF and four times within an intron (Table 1; Fig. 2). Furthermore, the insertion

**Table 1** Reinsertion sites of the transposable element *mimp1* in *Fusarium culmorum*. Sequence length, homology identity, distance (bp) upstream or downstream of a gene region in the *Fusarium graminearum* genome and predicted function are given.

| Revertant | Sequence length and identity (%) | *mimp1* location towards ORFs | >500 bp | <500 bp | ORF of gene | Intron of gene | Predicted function | Accession number |
|---|---|---|---|---|---|---|---|---|
| M7/1 | 970 bp (96.5%) | 3′ | | 152 bp to FGSG 11788 | | | Hypothetical protein | JQ710755 |
| M7/2 | 302 bp (95%) | 3′ | 1134 bp to FGSG 12526 | | | | Hypothetical protein | JQ710756 |
| M7/3 | 2335 bp (98%) | 5′ | | 437 bp to FGSG 11855 | | | Conserved hypothetical protein | JQ710757 |
| M7/7 | 852 bp (93%) | 5′ | | 29 bp to FGSG 09135 | | | Conserved hypothetical protein | JQ710758 |
| M7/8 | 852 bp (96%) | 5′ | 739 bp to FGSG 08710 | | | | Probable septin aspE | JQ710759 |
| M7/11 | 1093 bp (93%) | 5′ | | 143 bp to FGSG 02893 | | | Related to protein-arginine deiminase type II | JQ710760 |
| M7/15 | 913 bp (97%) | 5′ | 1118 bp to FGSG 08811 | | | | Translation elongation factor 1α | JQ710761 |
| M7/18 | 2599 bp (97%) | 3′ | | 493 bp to FGSG 17519 | | | Related to β-transducin-like protein | JQ710762 |
| 1A | 473 bp (98%) | 5′ | | 184 bp to FGSG 09610 | | | Conserved hypothetical protein | JQ710815 |
| 5A | 934 bp (96%) | 5′ | 971 bp to FGSG 11623 | | | | Conserved hypothetical protein | JQ710763 |
| 6A | 586 bp (96%) | 5′ | | 286 bp to FGSG 06546 | | | Conserved hypothetical protein | JQ710764 |
| 8A | 1061 bp (94%) | 5′ | 1609 bp to FGSG 16595 | | | | Probable phosphoglyceromutase | JQ710765 |
| 9A | 1607 bp (98%) | 5′ | 1254 bp to FGSG 16476 | | | | Hypothetical protein | JQ710766 |
| 11A | 994 bp (98%) | | | | FGSG 00620 | | Probable ammonium transporter MEPa | JQ710767 |
| 13A | 1168 bp (94%) | 5′ | 1173 bp to FGSG 02128 | | | | Conserved hypothetical protein | JQ710768 |
| Y4 | 450 bp (98%) | | | | FGSG 05107 | | Conserved hypothetical protein | JQ710770 |
| Y6 | 364 bp (94%) | 5′ | 1476 bp to FGSG 10135 | | | | Conserved hypothetical protein | JQ710769 |
| Y9 | 613 bp (97.5%) | | | | FGSG 13553 | | Hypothetical protein | JQ710771 |
| Y11 | 636 bp (97%) | 5′ | | 159 bp to FGSG 15384 | | | Hypothetical protein | JQ710772 |
| Y15 | 279 bp (98%) | 3′ | 1530 bp to FGSG 13051 | | | | Hypothetical protein | JQ710773 |
| Y16 | 574 bp (89%) | 5′ | 2132 bp to FGSG 00140 | | | | Related to ankyrin 3 | JQ710774 |
| Y19 | 387 bp (97%) | 5′ | 708 bp to FGSG 00279 | | | | Conserved hypothetical protein | JQ710775 |
| Y20 | 333 bp (95%) | 3′ | 4037 bp to FGSG 05037 | | | | Conserved hypothetical protein | JQ710776 |
| Y22 | 798 bp (95%) | 5′ | | 297 bp to FGSG 06060 | | | Related to ferric reductase FRE2 precursor | JQ710777 |
| Y25 | 1089 bp (98%) | 5′ | | 430 bp to FGSG 06980 | | | Hypothetical protein | JQ710778 |
| Y26 | 506 bp (96%) | | | | | FGSG 09054 | Related to dimethylaniline monooxygenase | JQ710779 |
| Y27 | 410 bp (97%) | 5′ | 1820 bp to FGSG 00846 | | | | Related to suppressor protein PSP1 | JQ710780 |
| Y28 | 798 bp (92%) | 3′ | 638 bp to FGSG 09913 | | | | Related to dityrosine transporter | JQ710781 |
| Y29 | 626 bp (98%) | 5′ | 1536 bp to FGSG 09716 | | | | Related to DNA repair protein rhp55 | JQ710782 |
| Y30 | 711 bp (93%) | | | | FGSG 03409 | | Related to L-fucose permease | JQ710783 |
| Y32 | 411 bp (92%) | 3′ | 811 bp to FGSG 09882 | | | | Related to short-chain alcohol dehydrogenase | JQ710784 |

 

**Table 1** Contiuned.

| Revertant | Sequence length and identity (%) | *mimp1* location towards ORFs | >500 bp | <500 bp | ORF of gene | Intron of gene | Predicted function | Accession number |
|---|---|---|---|---|---|---|---|---|
| Y33 | 1158 bp (98%) | | | | | FGSG 11910 | Hypothetical protein | JQ710785 |
| Y107 | 825 bp (97%) | 5′ | | 50 bp to FGSG 13619 | | | Conserved hypothetical protein | JQ710786 |
| Y108 | 1241 bp (98%) | | | | FGSG 10216 | | Related to potassium channel β-subunit protein | JQ710787 |
| Y111 | 703 bp (97%) | 3′ | 1613 bp to FGSG 06651 | | | | Conserved hypothetical protein | JQ710789 |
| Y112 | 526 bp (98.5%) | 5′ | | 493 bp to FGSG 05677 | | | Conserved hypothetical protein | JQ710788 |
| Y113 | 1109 bp (98%) | 3′ | 1576 bp to FGSG 13909 | | | | Hypothetical protein | JQ710790 |
| Y116 | 693 bp (98%) | 3′ | | 417 bp to FGSG 13305 | | | Hypothetical protein | JQ710792 |
| Y119 | 737 bp (96%) | | | | FGSG 04993 | | Conserved hypothetical protein | JQ710791 |
| Y120 | 382 bp (98%) | 3′ | 1863 bp to FGSG 09523 | | | | Conserved hypothetical protein | JQ710793 |
| Y121 | 419 bp (96%) | | | | | FGSG 15840 | Hypothetical protein | JQ710794 |
| Y122 | 773 bp (96%) | 3′ | 788 bp to FGSG 05046 | | | | Conserved hypothetical protein | JQ710795 |
| Y124 | 338 bp (96%) | 5′ | | 419 bp to FGSG 06297 | | | Related to protein tyrosine phosphatase φ | JQ710796 |
| Y126 | 797 bp (98%) | 3′ | 1683 bp to FGSG 00605 | | | | Conserved hypothetical protein | JQ710797 |
| Y127 | 488 bp (98%) | | | | FGSG 02321 | | Oxidoreductase that catalyses the conversion of dimeric 9-hydroxyrubrofusarin to aurofusarin | JQ710798 |
| Y130 | 679 bp (98%) | 5′ | 1520 bp to FGSG 09717 | | | | Related to RING3 kinase | JQ710799 |
| Y131 | 930 bp (96%) | 5′ | | 496 bp to FGSG 07390 | | | Conserved hypothetical protein | JQ710800 |
| Y132 | 638 bp (87%) | 5′ | | 461 bp to FGSG 08130 | | | Conserved hypothetical protein | JQ710801 |
| Y134 | 559 bp (98%) | 5′ | 1136 bp to FGSG 01307 | | | | Related to GATA transcription factor | JQ710802 |
| Y135 | 522 bp (97%) | 5′ | | 298 bp to FGSG 17290 | | | Hypothetical protein | JQ710803 |
| Y201 | 665 bp (92%) | 5′ | | 278 bp to FGSG 04913 | | | Related to β-glucosidase | JQ710804 |
| Y203 | 554 bp (99%) | | | | FGSG 05897 | | Conserved hypothetical protein | JQ710805 |
| Y261 | 995 bp (98%) | 3′ | 3316 bp to FGSG 13126 | | | | Hypothetical protein | JQ710806 |
| Y336 | 1301 bp(98.5%) | 3′ | 1718 bp to FGSG 11775 | | | | Hypothetical protein | JQ710807 |
| Y420 | 516 bp (98%) | | | | FGSG 01325 | | Conserved hypothetical protein | JQ710808 |
| Y424 | 2040 bp (98%) | 5′ | | 209 bp to FGSG 09682 | | | Conserved hypothetical protein | JQ710809 |
| Y558 | 624 bp (98%) | | | | | FGSG 13050 | Hypothetical protein | JQ710810 |
| Y560 | 1075 bp (96%) | 5′ | 1372 bp to FGSG 09422 | | | | Related to C-terminal of *Aspergillus nidulans* regulatory protein (qutR) | JQ710811 |
| Y562 | 1041 bp (97%) | | | | FGSG 02115 | | Related to TRI7 trichothecene biosynthesis gene cluster | JQ710812 |
| 12A | 1526 bp | No significant similarity found in any *Fusarium* genome currently sequenced | | | | | | JQ710813 |
| M7/14 | 1001 bp | High homology with *F. verticillioides* 7600 and *F. oxysporum* 4287 | | | | | Hypothetical protein | JQ710814 |

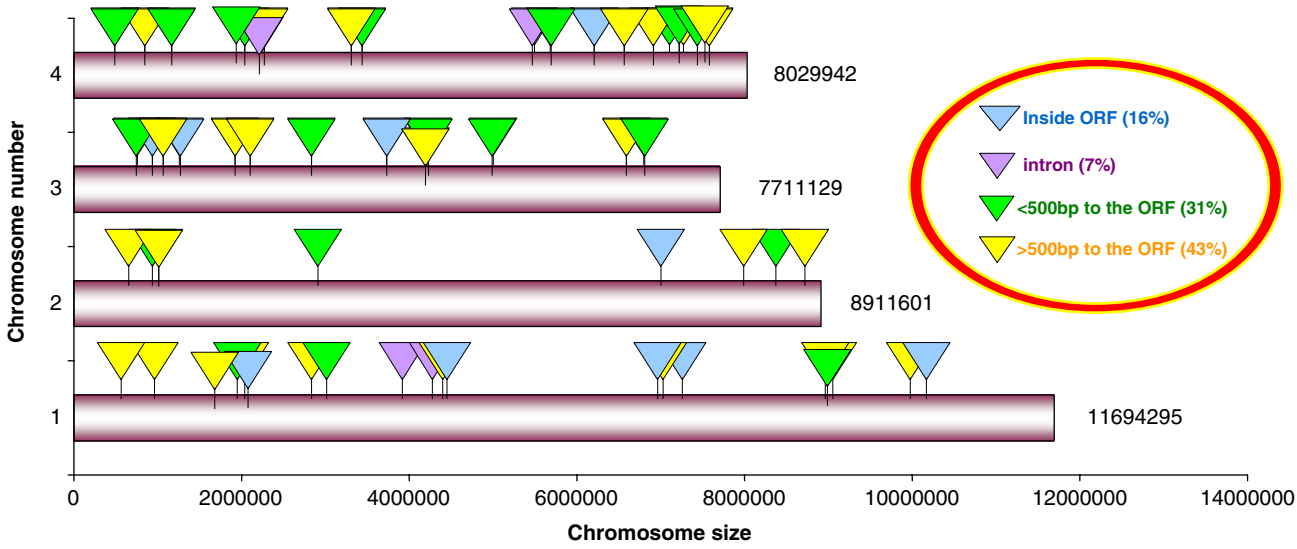


**Fig. 2** Putative localization of the distribution of *mimp1* reinsertion sites in the closest genome available to *F. culmorum: Fusarium graminearum* (*Gibberella zeae*). The transposon reinserted evenly in all four chromosomes of *G. zeae* and was located in 23% of the analysed flanking regions within an open reading frame (ORF) or an intron.

sites of *mimp1* in the *F. graminearum* genome were observed for 19 times at less than 500 bp (upstream or downstream) of a genic region, 20 times at a distance greater than 1000 bp and six times between 1000 and 500 bp (Table 1; Fig. 2). The identity between *F. culmorum* sequences and the *F. graminearum* genome, determined as a percentage, was 96%, indicating conserved protein structure and function. Only two flanking sequences did not show any homology with the *F. graminearum* genome. The flanking sequence of revertant M7/14 showed homology with the *F. verticillioides* 7600 genome and, to a lesser extent, with the *F. oxysporum* 4287 genome, whereas one of the sequences (revertant 12A) displayed no homology with any previously sequenced *Fusarium* genome, suggesting that it may represent a specific putative sequence of *F. culmorum* (Table 1). The *mimp1* transposon was inserted within or near a gene encoding a 'hypothetical protein' or 'conserved hypothetical protein' in most tested cases. One *mimp1* reinsertion (revertant Y127) was in the homologue of the *aurO* gene, one of the 11 genes involved in the biosynthetic process of aurofusarin with rubrofusarin as an intermediate in *F. graminearum* (Table 1) (Frandsen *et al*., 2006, 2011). The *mimp1* insertion interrupted the production of aurofusarin, determining a shift of the colony colour towards yellow–orange (Fig. S4, Supporting Information), which is a result of the shift of the rubrofusarin/aurofusarin ratio (Frandsen *et al*., 2006; Malz *et al*., 2005), thus verifying the efficiency of *mimp1* in inactivating gene function.

To identify other phenotypes related to the insertion of *mimp1* in ORFs, 10 revertants (Table 1) were grown on different substrates [complete medium (CM; Correll *et al*., 1987) amended with 1 M sorbitol and CM amended with 0.7% NaCl (for osmotic stress), CM amended with 0.01% sodium dodecylsulphate (SDS) and CM amended with 0.02% $H_2O_2$ (for oxidative stress)]. Ten microlitres of a conidial suspension ($10^5$ conidia/mL) were inoculated in the middle of Petri dishes. To test for thermal stress resistance, the strains were cultured on potato dextrose agar (PDA) at 33 °C (maximum level tolerated by *F. culmorum*) in the dark for 10 days. After inoculation, the Petri dishes were incubated at 22 °C with a photoperiod of 12 h for 3–5 days. The growth of each revertant was estimated by measuring the colony diameter. All experiments were conducted in triplicate at least twice, and a one-way analysis of variance, followed by multiple comparison applying Dunnett's test, was performed using Minitab® for Windows release 12.1 software.

No temperature-resistant mutants could be identified. However, the system *mimp1/impala* allowed the identification of the genes involved in metabolic processes that alter the phenotype of some revertants growing under different stress conditions (osmotic and oxidative stress). Revertants Y4 and Y203 were altered in their growth properties when cultivated under oxidative stress conditions: both showed a significant increase in growth diameter after 3 days of incubation at room temperature (Y4 = 3.0 $\pm$ 0.0 cm; Y203 = 2.37 $\pm$ 0.40 cm) compared with the reference strain M7 (1.30 $\pm$ 0.20 cm; Fig. S5, Supporting Information).

Bioinformatics analysis showed that, in revertant Y4, *mimp1* was inserted within a gene homologous to *F. graminearum* (FGSG 05107) containing a transmembrane domain conserved in other fungi, but not present in yeast. *Fusarium graminearum* protein subcellular localization (FGsub) analysis (Sun *et al*., 2010) suggested FGSG 05107 to be a Golgi or endosome protein. Flanking region analysis of Y203 allowed the identification of

 

a conserved hypothetical protein homologous to *Saccharomyces cerevisiae YFL061w*, a protein with a metal-dependent phosphohydrolase domain expressed in yeast and conserved in all fungi. The function is unknown in pathogenic fungi and no secure localization for this gene could be predicted using both FGsub and Interpretable Subcellular Localization Prediction (YLoc; http://abi.inf.uni-tuebingen.de/Services/YLoc/webloc.cgi) (Briesemeister *et al*., 2010), making this gene interesting for future functional characterization.

To determine whether the trans-activated *mimp1* element moved into a promoter region or into a putative ORF involved in the pathogenic process necessary to cause CFR disease, the 1300 revertants were tested on durum wheat seedlings by placing 10 plugs of mycelium, each bearing one seed of durum wheat (*Triticum durum* cv. Claudio, kindly provided by Unità di Ricerca per la Valorizzazione Qualitativa dei Cereali, CRA-QCE, Rome, Italy), into a plastic sowing pot and covering with sterile soil. Pathogenicity tests were conducted in a glasshouse at 25–30 °C and, 3 weeks after inoculation, the severity of disease was assessed using the McKinney index (Balmas *et al*., 2006; McKinney, 1923). Revertants showing a McKinney index below 60% during a first pre-screening were tested again in three replicates of 10 plugs each. The emergence of young seedlings and the severity of disease were monitored weekly during 4 weeks from sowing. The disease trend was evaluated by one-way analysis of variance, followed by multiple comparison applying Dunnett's test.

In preliminary screening, only a small group of 32 revertants showed a moderate reduction in disease incidence, which was related to higher seedling emergence. The weekly trend of two subsequent independent experiments did not confirm such a delay in symptom appearance, which was related to slower seedling emergence, but this difference was definitely reduced at the third to fourth week (Fig. S6, Supporting Information). Therefore, no *mimp1* insertion could be linked unequivocally to the pathogenic phenotype under high disease pressure.

All the flanking sequences were deposited in the Genome sequence Service database from the National Center for Biotechnology Information (NCBI) (http://www.ncbi.nlm.nih.gov/dbGSS/), and mutants are available on request for further functional studies.

To conclude, our results show that the transposon tagging approach based on the *mimp1/impala* double-component system is an efficient method to randomly mark genes in *F. culmorum*, as it allowed us to map genes and gene sequences not yet described in this genetic context. In addition, this is a powerful mutagenesis tool, which is useful for the functional analysis of the *F. culmorum* genome. Further validation of the double-component system will be performed once the complete genome sequence is available in order to understand the role and function of tagged genes with respect to the pathogenicity and mycotoxigenic potential of this pathogen.

## ACKNOWLEDGEMENTS

This work was funded by the Ministry of University and Research (PRIN 2007: Transposon tagging and RNA silencing in the wheat pathogen *Fusarium culmorum*) and by Regione Autonoma della Sardegna (Legge Regionale 7 agosto 2007, n. 7 'Promozione della ricerca scientifica e dell'innovazione tecnologica in Sardegna'). F.S. acknowledges receipt of a PhD fellowship (XXIV cycle) sponsored by AGRIS SARDEGNA – Agenzia per la Ricerca in Agricoltura. The Fond National de la Recherche of Luxembourg is acknowledged.

## REFERENCES

**Balmas, V., Delogu, G., Esposito, S., Rau, D. and Migheli, Q.** (2006) Use of a complexation of tebuconazole with β-cyclodextrin for controlling foot and crown rot of durum wheat incited by *Fusarium culmorum*. *J. Agric. Food Chem.* **54**, 480–484.

**Beccari, G., Covarelli, L. and Nicholson, P.** (2011) Infection processes and soft wheat response to root rot and crown rot caused by *Fusarium culmorum*. *Plant Pathol.* **60**, 671–684.

**Briesemeister, S., Rahnenführer, J. and Kohlbacher, O.** (2010) Yloc – an interpretable web server for predicting subcellular localization. *Nucleic Acids Res.* **38**, W497–W502.

**Carr, P.D., Tuckwell, D., Hey, P.M., Simon, L., d'Enfert, C., Birch, M., Oliver, J.D. and Bromley, M.J.** (2010) The transposon *impala* is activated by low temperatures: use of a controlled transposition system to identify genes critical for viability of *Aspergillus fumigatus*. *Eukaryot. Cell*, **9**, 438–448.

**Correll, J.C., Klittich, C.J.R. and Leslie, J.F.** (1987) Nitrate non-utilizing mutants of *Fusarium oxysporum* and their use in vegetative compatibility tests. *Phytopathology*, **77**, 1640–1646.

**Dufresne, M., Hua-Van, A., Abd el Wahab, H., Ben M'Barek, S., Vasnier, C., Teysset, L., Kema, G.H.J. and Daboussi, M.J.** (2007) Transposition of a fungal MITE through the action of a Tc1-like transposase. *Genetics*, **175**, 441–452.

**Dufresne, M., van der Lee, T., Ben M'Barek, S., Xu, X., Zhang, X., Liu, T., Waalwijk, C., Zhang, W., Kema, G.H.J. and Daboussi, M.J.** (2008) Transposon-tagging identifies novel pathogenicity genes in *Fusarium graminearum*. *Fungal Genet. Biol.* **45**, 1552–1561.

**Frandsen, R.J.N., Nielsen, N.J., Maolanon, N., Sørensen, J.C., Olsson, S., Nielsen, J. and Giese, H.** (2006) The biosynthetic pathway for aurofusarin in *Fusarium graminearum* reveals a close link between the naphthoquinones and naphthopyrones. *Mol. Microbiol.* **61**, 1069–1080.

**Frandsen, R.J.N., Schutt, C., Lund, B.W., Staerk, D., Nielsen, J., Olsson, S. and Giese, H.** (2011) Two novel classes of enzymes are required for the biosynthesis of aurofusarin in *Fusarium graminearum*. *J. Biol. Chem.* **286**, 10 419–10 428.

**Goswami, R.S. and Kistler, H.C.** (2004) Heading for disaster: *Fusarium graminearum* on cereal crops. *Mol. Plant Pathol.* **5**, 515–525.

**Hua-Van, A., Davière, J.M., Langin, T. and Daboussi, M.J.** (2000) Genome organization in *Fusarium oxysporum*: clusters of class II transposons. *Curr. Genet.* **37**, 339–347.

**Malardier, L., Daboussi, M.J., Julien, J., Roussel, F., Scazzochio, C. and Brygoo, Y.** (1989) Cloning of the nitrate reductase gene (*niaD*) of *Aspergillus nidulans* and its use for transformation of *Fusarium oxysporum*. *Gene*, **78**, 147–156.

**Malz, S., Grell, M.N., Thrane, C., Maier, F.J., Rosager, P., Felk, A., Albertsen, K.S., Salomon, S., Bohn, L., Schäfer, W. and Giese, H.** (2005) Identification of a gene cluster responsible for the biosynthesis of aurofusarin in the *Fusarium graminearum* species complex. *Fungal Genet. Biol.* **42**, 420–433.

**McKinney, H.H.** (1923) Influence of soil temperature and moisture on infection of wheat seedlings by *Helminthosporium sativum*. *J. Agric. Res.* **26**, 195–217.

**Mishra, P.K., Fox, R.T.V. and Culham, A.** (2003) Intersimple sequence repeat and aggressiveness analyses revealed high genetic diversity, recombination and long-range dispersal in *Fusarium culmorum*. *Ann. Appl. Biol.* **143**, 291–301.

**Potter, C.J. and Luo, L.** (2010) Splinkerette PCR for mapping transposable elements in *Drosophila*. *Plos ONE*, **5**, e10168.

**Scherm, B., Orrù, M., Balmas, V., Spanu, F., Azara, E., Delogu, G., Hammond, T.M., Keller, N.P. and Migheli, Q.** (2011) Altered trichothecene biosynthesis in *TRI6*-silenced transformants of *Fusarium culmorum* influences the severity of crown and foot rot on durum wheat seedlings. *Mol. Plant Pathol.* **12**, 759–771.

**Sudakin, D.L.** (2003) Trichothecenes in the environment: relevance to human health. *Toxicol. Lett.* **143**, 97–107.

**Sun, C., Zhao, X.M., Tang, W. and Chen, L.** (2010) FGsub: *Fusarium graminearum* protein subcellular localizations predicted from primary structures. *BMC Syst. Biol.* **4**, S2–S12.

**Wagacha, J.M. and Muthomi, J.W.** (2007) *Fusarium culmorum*: infection process, mechanisms of mycotoxin production and their role in pathogenesis in wheat. *Crop Prot.* **26**, 877–885.

## SUPPORTING INFORMATION

Additional Supporting Information may be found in the online version of this article:

**Fig. S1** Co-transformation outline. Fungal protoplasts, obtained from macroconidia and young thalli of *Fusarium culmorum* MCf 21 nit1 grown on potato dextrose agar (PDA), were purified and used directly in fungal co-transformation with plasmids pNm1H18 and pHEO62. The plasmid pHEO62 carries the *impalaE* transposase, cloned between the *gpdA* promoter and the *trpC* terminator of *Aspergillus nidulans*, together with the *hph* selectable marker conferring resistance to hygromycin B. The plasmid pNm1H18 carries the *niaD*::*mimp1* construct. The *mimp1* transposon was inserted into the first intron of the *niaD* gene of *A. nidulans* in a *Hind*III restriction site. The exons are represented as green boxes, and introns as black lines. The transposition events are possible on the basis of the high similarity of the *mimp1* inverted repeat to those of the *impala* transposon.

**Fig. S2** Agarose gel electrophoresis of polymerase chain reaction (PCR) products obtained by primers niaD144 and niaD754r on three co-transformants and one respective revertant. The size expected for co-transformants is 717 bp, corresponding to the *niaD* gene carrying the *mimp1* element. Monocopy insertion is evidenced by a single band of 493 bp, suggesting excision of *mimp1*.

**Fig. S3** Insertion site preference of *mimp1* by a cut-and-paste mechanism into TA dinucleotides (black boxes). Alignments on the right (A) and on the left (B) flanking sequences of some revertants and *mimp1* partial sequence are shown.

**Fig. S4** *In vitro* growth of co-transformant M7 and of revertant Y127 cultured on complete medium (CM) containing 0.7% NaCl at room temperature for 5 days. Y127 develops a yellow–orange mycelium as a result of inactivation of the *aurO* gene by the *mimp1* transposable element.

**Fig. S5** Identification of oxidative resistant phenotypes on complete medium (CM) amended with 0.02% $H_2O_2$. After incubation at room temperature for 3 days, revertants Y4 and Y203 show a mycelium growth diameter greater than that of co-transformant M7.

**Fig. S6** Emergence of durum wheat seedlings (cv. Claudio) and Fusarium crown and root rot disease index (weekly trend). *Fusarium culmorum* M7 co-transformant and 32 *mimp1/impala* revertants were analysed to evaluate the emergence (A–E) and disease incidence (F–J) during 4 weeks. Noninoculated seeds were sown into a plastic sowing pot as control. After 3–4 weeks of incubation at 25 °C, differences between the M7 co-transformant and the revertants were reduced.

**Table S1** List of primers used to identify excision/reinsertion events of the transposable element *mimp1* by specific polymerase chain reaction (PCR) and Southern blotting experiments, and PCR conditions used for each primer pair.

**Table S2** List of primers used for splinkerette-polymerase chain reaction (sp-PCR). The primer pairs used to obtain the right flanking sequences of *mimp1* are as follows: SPLNK#1–M1Div53F for the first round of PCR, and SPLNK#2–SacF for the second round. Conversely, the left flanking sequences of the transposon were isolated using the primer pairs SPLNK#1–2R (round 1) and SPLNK#2–3R (round 2). The PCR product contains the flanks of genomic DNA of interest between the transposon *mimp1* insertion site and the specific enzyme restriction site.

**Table S3** Size and GC content comparison of the reinsertion sites of the transposable element *mimp1* in *Fusarium culmorum* with the corresponding sequences in the *Fusarium graminearum* genome.

Please note: Wiley-Blackwell are not responsible for the content or functionality of any supporting materials supplied by the authors. Any queries (other than missing material) should be directed to the corresponding author for the article.